ISSN 1674-1056
http://cpb.iphy.ac.cn
http://iopscience.iop.org/cpb
中国物理 B
Chinese Physics
中国物理 Chinese Physics B

Tunable plasmon induced transparency based on asymmetric H-shaped graphene metamaterials

Yu-Chen Tian(田雨宸), Wei Jia(贾微), Pei-Wen Ren(任佩雯), Chun-Zhen Fan(范春珍)

Citation: Chin. Phys. B . 2018, 27(12): 124205. **doi:** 10.1088/1674-1056/27/12/124205
Journal homepage: http://cpb.iphy.ac.cn; http://iopscience.iop.org/cpb

What follows is a list of articles you may be interested in

Carboxyl graphene oxide solution saturable absorber for femtosecond mode-locked erbium-doped fiber laser

Rui-dong Lv(吕瑞东), Lu Li(李璐), Yong-gang Wang(王勇刚), Zhen-dong Chen(陈振东), Si-cong Liu(刘思聪), Xi Wang(王茜), Jiang Wang(王江), Yong-fang Li(李永放)

Chin. Phys. B . 2018, 27(11): 114214. **doi:** 10.1088/1674-1056/27/11/114214

Surface plasmon polariton at the interface of dielectric and graphene medium using Kerr effect

Bakhtawar, Muhammad Haneef, B A Bacha, H Khan, M Atif

Chin. Phys. B . 2018, 27(11): 114215. **doi:** 10.1088/1674-1056/27/11/114215

Study on polarization properties of graphene coated D-shaped fiber

Xuejing Liu(刘学静), Luwen Yang(杨禄文), Jingyun Ma(马敬云), Caili Li(李彩丽), Wa Jin(金娃), Weihong Bi(毕卫红)

Chin. Phys. B . 2018, 27(10): 104206. **doi:** 10.1088/1674-1056/27/10/104206

Tunable graphene-based mid-infrared band-pass planar filter and its application

Somayyeh Asgari, Hossein Rajabloo, Nosrat Granpayeh, Homayoon Oraizi

Chin. Phys. B . 2018, 27(8): 084212. **doi:** 10.1088/1674-1056/27/8/084212

Generation and evolution of multiple operation states in passively mode-locked thulium-doped fiber laser by using a graphene-covered-microfiber

Xiao-Fa Wang(王小发), Jun-Hong Zhang(张俊红), Xiao-Ling Peng(彭晓玲), Xue-Feng Mao(毛雪峰)

Chin. Phys. B . 2018, 27(8): 084215. **doi:** 10.1088/1674-1056/27/8/084215

Tunable plasmon-induced transparency based on asymmetric H-shaped graphene metamaterials*

Yu-Chen Tian(田雨宸), Wei Jia(贾微), Pei-Wen Ren(任佩雯), and Chun-Zhen Fan(范春珍)†

School of Physical Science and Engineering, Zhengzhou University, Zhengzhou 450001, *China*

(Received 10 July 2018; revised manuscript received 29 August 2018; published online 10 November 2018)

We propose and numerically demonstrate a tunable plasmon-induced transparency (PIT) phenomenon based on asymmetric H-shaped graphene metamaterials. The tunable PIT effect is realized through varying the applied polarization angles rather than changing the structure geometry. By simply adjusting the polarization angle, the transmission spectra can be controlled between the switch-on state and switch-off state. The physical mechanism of the induced transparency is revealed from magnetic dipole inductive coupling and phase coupling. Importantly, by varying the Fermi energy of the graphene or the refractive index of the substrate, the resonant position of the PIT can be dynamically controlled and the maximum modulation depths can reach up to 60.7%. The sensitivity (nm/RIU) of the graphene structure, which is the shift of resonance wavelength per unit change of refractive index, is 5619.56 nm/RIU. Moreover, we also extend our research to the x-axis symmetric H-shaped structure, and the tunable PIT transmission window can also be realized. The physical mechanism of the induced transparency is revealed from the electric dipole hybridization coupling. Our designed H-shaped graphene-based structures is a promising candidate for compact elements such as tunable sensors, switches and slow-light devices.

Keywords: plasmon-induced transparency, graphene, polarization, optical filter

PACS: 42.50.Gy, 78.67.Pt, 61.48.Gh **DOI:** 10.1088/1674-1056/27/12/124205

1. Introduction

Electromagnetically induced transparency (EIT) is a quantum interference phenomenon in the weak electromagnetic field under the effect of a strong driving electromagnetic field in the atomic system.[1–3] This results in a narrow window in the transmission spectrum. The plasmon-induced transparency (PIT), an EIT-like effect, has attracted attention due to its significant advantages and wide practical applications,[4,5] such as in sensors,[6–9] optical storage,[10–12] optical switches, and so on.[13–16] However, for metal metamaterials, once the PIT devices have been fabricated, the transmission window is very difficult to tune except by accurately changing the geometry of structures, which limits the performance and repeatability of designated PIT sample. Recently, graphene has been introduced into the design of PIT devices due to its unique optical and electrical properties.[17–19] It exhibits the characteristic of the flexible tunability, the extreme field confinement and low propagation loss, especially the gate-voltage-dependent feature that the Fermi energy (E_F) of graphene can be tuned dynamically by using the external electrostatic gating.[20,21]

Hence, graphene can be considered as a new class of active plasmonic material for application in photonic devices. Fu *et al.* proposed a novel disk-strip hybrid graphene nanostructure to achieve PIT resonance that has a large positive group delay in the vicinity of the resonant transparency window.[22] They also presented two parallel graphene nanostrips that can be used as a localized surface plasmon resonance sensor in the mid-infrared region.[23] Luo *et al.* achieved PIT effects based on the strong coupling between localized and propagating plasmonic mode in layered graphene ribbon-grating and continuous sheet systems.[24] Zhang *et al.* have studied the tunable PIT with graphene-array metasurface.[25] Compared with this research, we have systematically investigated the tunable PIT effect through varying the polarization angle and the fermi energy, which makes manipulating of the PIT system more effective and contactless. We also compared the application of the designed structure in sensitivity with those of other structures.

In this paper, we propose the self-asymmetric H-shaped graphene metamaterial to achieve the PIT effect. Interestingly, the modulation of the PIT transparency window can be achieved by varying the polarization angles rather than changing the structure geometry parameters. Owing to the unique properties of graphene, the resonant transparency window can be dynamically tuned by the Fermi energy. Moreover, the sensitivity of 5619.26 nm/RIU is achieved in the proposed structure based on the sensitivity measurements with different dielectric substrates. The physical mechanism of the induced transparency is revealed with magnetic dipole inductive coupling and phase coupling. We also extend our research to the *x*-axis symmetric H-shaped graphene metamaterial, and the PIT

*Project supported by the Key Science and Technology Research Project of Henan Province, China (Grant Nos. 162102210164 and 1721023100107) and the Natural Science Foundation of Henan Educational Committee, China (Grant No. 17A140002).

†Corresponding author. E-mail: chunzhen@zzu.edu.cn

© 2018 Chinese Physical Society and IOP Publishing Ltd

effect can also be tuned through varying the polarization angle and the fermi energy. However, the underlying mechanism is the detuning of two bright modes.

2. Metamaterial design and simulation methods

The designed asymmetric H-shaped graphene structure with a 7×7 cell array is shown in Fig. 1(a). The unit cell includes graphene pattern layer and dielectric layer, as indicated in Fig. 1(b). The detailed structural parameters are marked in the diagram, where $P_x = P_y = 8$ μm, $l_1 = 5.6$ μm, $l_2 = 2.3$ μm, $w_1 = 0.6$ μm, and $t_1 = 3$ μm. The top view of the unit cell with $l_3 = 0.8$ μm and $l_4 = 1.5$ μm is shown in Fig. 1(c). The dashed-line is the symmetry axis of l_1. A linearly polarized plane wave light normally is incident along the z-axis direction and the angle of the polarization direction with respect to the x axis is defined as θ. Both the transmission spectrum and the field distribution are calculated by using COMSOL Multiphysics software, which is commercial software that is based on the finite element method. The computation domain consists of only a unit cell with the perfectly matched layer applied to the boundary along the propagation direction (z axis) and periodic condition imposed on the four lateral boundaries in x and y directions.

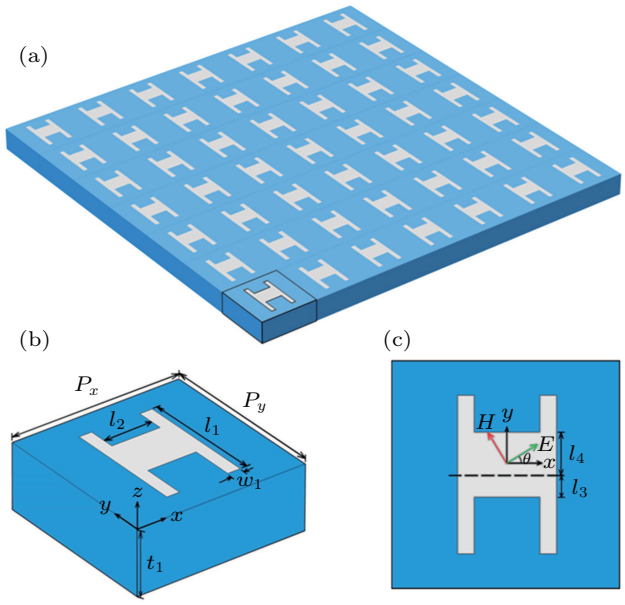


Fig. 1. (color online) Proposed H-shaped asymmetric structure along y axis, showing (a) overview of a 7×7 cells array, (b) schematic view of graphene nanostructure on substrate with dielectric coefficient 3.9, where $P_x = P_y = 8$ μm, $l_1 = 5.6$ μm, $l_2 = 2.3$ μm, $w_1 = 0.6$ μm, and $t_1 = 3$ μm, and (c) top view of graphene nanostructure, where $l_3 = 0.8$ μm, and $l_4 = 1.5$ μm, and θ is the polarization angle.

In the simulations, graphene is modelled as a conductive surface.[17,26,27] The transition boundary condition is used for graphene and its thickness is set to be 1 nm. The conductivity of graphene can be derived in the random-phase approximation (RPA) in the local limit, and expressed as[19,28,29]

$$\sigma(\omega) = \frac{2e^2 k_B T}{\pi\hbar^2}\frac{\mathrm{i}}{\omega + \mathrm{i}\tau^{-1}}\ln\left[2\cosh\left(\frac{E_F}{2k_B T}\right)\right] + \frac{e^2}{4\hbar}\left[\begin{array}{l}\frac{1}{2} + \frac{1}{\pi}\arctan\left(\frac{\hbar\omega - 2E_F}{2k_B T}\right) \\ -\frac{\mathrm{i}}{2\pi}\ln\frac{(\hbar\omega + 2E_F)^2}{(\hbar\omega - 2E_F)^2 + 4(k_B T)^2}\end{array}\right], \quad (1)$$

where k_B is the Boltzmann constant, T is the temperature, ω is the frequency of light, τ is the carrier relaxation lifetime, and E_F is the Fermi energy. In our simulation, our method mainly focuses on the material effect in two-dimensional (2D) flat surface while ignoring that in out-of-plane direction. At the room temperature and low THz frequency ($E_F \gg k_B T, E_F \gg \hbar\omega$), the in-plane conductivity of the graphene can be represented by a Drude model:[30,31]

$$\sigma(\omega) = \frac{e^2 E_F}{\pi\hbar^2}\frac{\mathrm{i}}{\omega + \mathrm{i}\tau^{-1}}. \quad (2)$$

The intrinsic relaxation time is expressed as $\tau = \mu E_F / e v_F^2$ where $\mu = 10^4$ cm^{-1}·V^{-1}·s^{-1} is the measured DC mobility and v_F is the Fermi velocity.[32]

Electron-beam lithography and isotropic plasma etching are used to pattern graphene nanostructures.[33] To obtain the graphene metamaterial structures, a uniform single layer of graphene needs to be prepared at first. It can be obtained through mechanically extracted from bulk graphite crystals,[34] thermal decomposition of Sic,[35] and chemical vapor deposition method.[36] The most common method is chemical vapor precipitation, which produces a graphene layer with high conductivity and field-effect mobility. For the preparation of graphene nanostructures, electron beam lithography is very popular because of its high resolution; usually reaching up to 3 nm to 8 nm.[37] Recently, anisotropic etching has been proposed as a key technique for controllable graphene edge fabrication with atomic precision. Yang *et al.* reported a dry, anisotropic etching method of preparing the graphite and graphene. They are able to control the etching from the edges by tuning etching parameters such as plasma intensity, temperature, and duration.[38] Similarly, the asymmetric H-shaped graphene can be prepared through the following steps: first, a graphene layer synthesized with chemical vapor deposition is transferred to the substrate. Secondly, the H-shaped graphene array is completed by electron beam lithography. Then, the ion gel can be utilized as the top gate, while the bottom of substrate is used as the back gate. Finally, the carrier density in graphene can be changed by adjusting the voltage, and then the conductivity of graphene can be dynamically adjusted.

3. Results and discussion

Figures 2(a)–2(e) show the transmission spectra of H-shaped graphene structure with different values of polarization angle θ. When $\theta = 0°$, the electric field is along the x direction and the transmission spectrum exhibits a significant PIT

effect. A transparency peak located at position 2 (2.18 THz) appears between two resonance dips at position 1 (1.91 THz) and position 3 (2.46 THz). As θ increases, the transparency peak gives rise to a minor shift and the intensity decline at the same time. Finally, a transmission dip at 2.28 THz is obtained and the transparency window disappears at $\theta = 90°$. Thus, the transmission peak intensity is able to change from the switch-on state to the switch-off state with polarization angle θ varying from 0° to 90°. This actively tunable PIT effect implies its potential applications in making optical switches at THz frequencies.

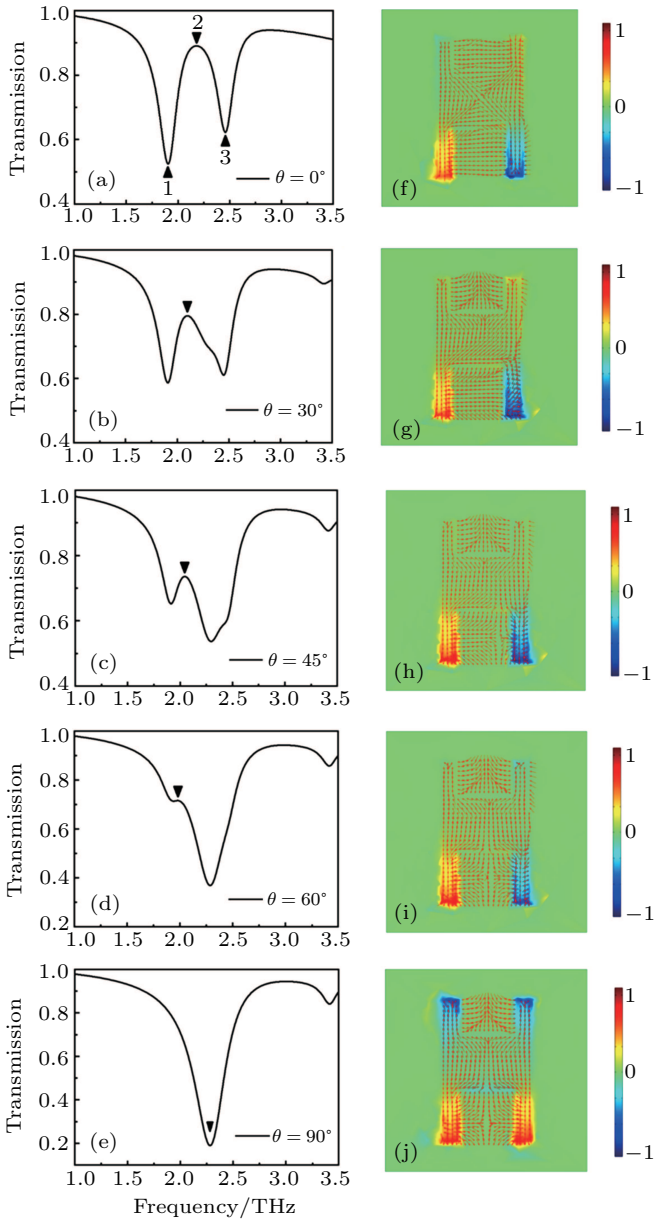


Fig. 2. (color online) (a)–(e) Transmission spectra of H-shaped graphene structure at different values of polarization angle θ, where $l_4 = 1.5$ μm and $E_F = 0.5$ eV. (f)–(j) Normalized electric field and normalized surface current distributions at resonant peak position, which are denoted by black arrows in panels (a)–(e).

To fully dig out the origin of such a PIT phenomenon, the normalized electric field distribution and normalized surface current distribution (in arrows) are given in Figs. 2(f)–2(j). For $\theta = 0°$, the electric field distribution of the upper part and the lower part are out-phase (similar to a quadrupole). The surface currents emerge clockwise on both sides. With the increase of polarization angle θ, the direction of the surface current gradually changes from the crossed distribution (Fig. 2(f)) to the same direction (Fig. 2(j)). This is a typical dipole mode at the resonance dip (2.28 THz) due to a parallel electric field to the arms of the structure. Briefly, the electric field distribution changes from a quadrupole to a couple of dipoles when the polarization angle is tuned from 0° to 90°. Namely, the PIT mode can be excited at $\theta = 0°$. By further enlarging the polarization angle θ, the PIT mode fades gradually and the dipole mode is enhanced.

To better reveal the mechanism of PIT resonance in our proposed structure, we investigate the electric field and normalized surface current distributions at 0° polarization angle. The results are shown in Fig. 3. The low frequency resonance dip 1 at 1.9 THz dominantly arises from the lower part, which is in accordance with the excited electric field as shown in Fig. 3(a). The resonance on the upper part evokes the high frequency resonance dip 3 at 2.46 THz, because the upper length is shorter than the lower one. In a sense, the upper part is regarded as dark-mode due to out-phase electric field with the excited electric field, while the lower is bright-mode because of its in-phase electric field with the excited electric field. At transparency frequency 2.18 THz, the destructive interference occurs between two modes and the electric field intensity is obviously lower than that of single mode excitation in Fig. 3(b). It can also be explained by magnetic dipole induced transparency mechanism in Fig. 4. The solid arrows represent the directions of the flowing currents and the marked μ represents the magnetic dipole moment. The circulating current is excited by incident field and gives rise to a magnetic dipole moment perpendicular to the x–y plane.[39,40] A single magnetic dipole moment coupled with the incident wave, and then a transmission dip is formed, such as 1.9 THz (ω_1) and 2.46 THz (ω_3). At transparency frequency 2.18 THz (ω_2), the currents of the upper part keep constant, while the currents of the lower flow in the anti-clockwise direction. Thus, the two dipole moments are aligned to be parallel and repulsive to each other, giving rise to a magnetic response in the system. Consequently, it enhances the propagation waves passing through at resonance.

In addition, it should be pointed out that the optical properties of graphene can be substantially modified via doping or gating since the conductivity of graphene depends strongly on Fermi energy. We can dynamically tune the transparency window over a broad wavelength range by controlling the Fermi energy levels of graphene. The results are shown in Fig. 5. Figure 5(a) shows the transmission spectra of the proposed graphene structure under different Fermi energies in the case

of $\theta = 0°$. It is found that as the Fermi energy increases, the transparency peak shifts to higher frequency. Meanwhile, the transmissions of two resonance dips are significantly reduced. The relationship between the resonant peak and the Fermi energy is shown in Fig. 5(b). The linear fit of the resonant peak in red line indicates that the larger Fermi energy causes a blueshift of the resonant peak. When the Fermi energy of graphene is 0.5 eV, the transmission peak is located at 2.18 THz. Increasing the Fermi energy to 0.9 eV, the location of the transmission peak moves to 2.89 THz. It is revealed that the transparency window can be tuned easily over a broad range in the investigated frequency regime only by a small change in the Fermi energy. It has a great potential application in optical filter. With $E_F = 0.7$ eV, the transmission intensity can reach 0.89 at 2.55 THz. When the Fermi energy of graphene increases to 0.9 eV, the transmission intensity declines sharply to 0.35. The maximum modulation depth of the metamaterial (MD $= |T_{max} - T_{min}|/T_{max}$) at 2.55 THz is 60.7%.

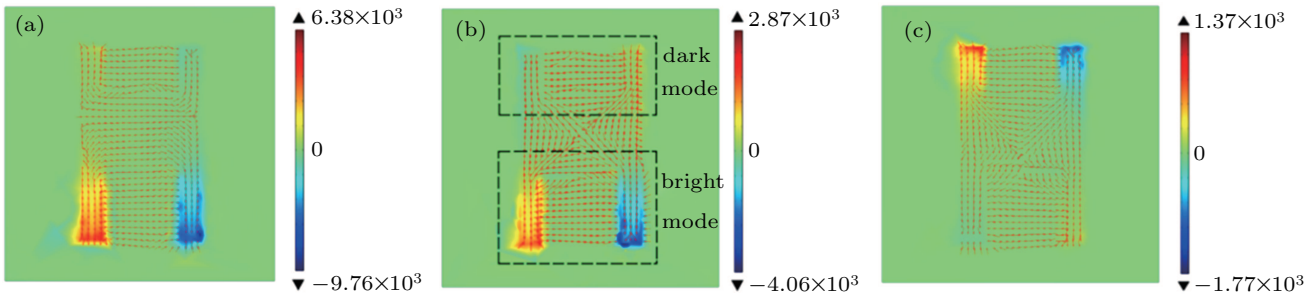


Fig. 3. (color online) Electric field and normalized surface current distributions at 0° polarization angle in Fig. 2(a) at three different resonant positions: (a) the first resonant position 1.9 THz (ω_1), (b) the second resonant position at 2.18 THz (ω_2), and (c) the third resonant position at 2.46 THz (ω_3).

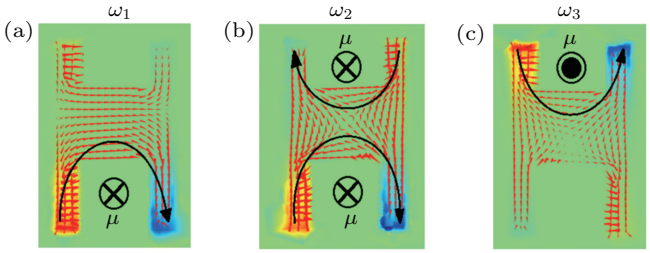


Fig. 4. (color online) Surface currents excited by magnetic-dipole coupling with the propagation waves.

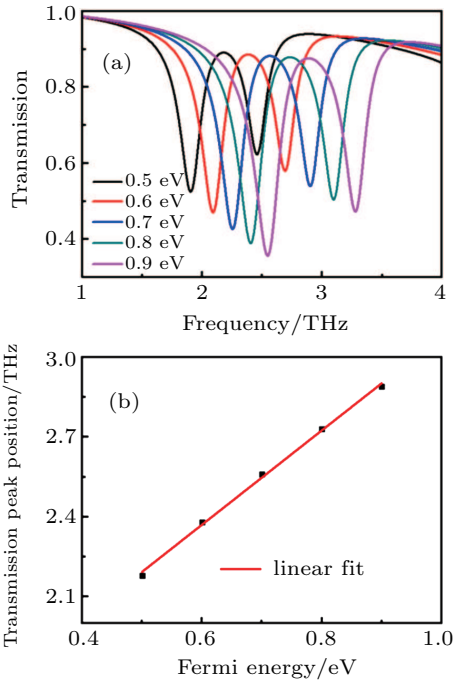


Fig. 5. (color online) (a) Transmission spectra of graphene based PIT structure under normal incidence at different values of E_F, and (b) relationship of the resonant PIT peak with Fermi energy E_F.

To explore the sensing ability of our proposed structure, figure 6(a) shows that the PIT spectra are changed with different refractive indexes n of the substrate under normal incident electromagnetic wave and other material parameters are unchanged. With refractive index increasing from 1.7 to 2.1, the transparency window is obviously red-shifted and the resonance strength of the PIT window is slightly enhanced. The relationship between the resonant peak and the refractive index is shown in Fig. 6(b). It can be clearly found that small perturbations can result in dramatic shift of the resonance. A spectral shift relative to the refractive index n of the substrates is plotted in Fig. 6(c). The sensitivity of the structure can be calculated with the linear fitting of 5619.26 nm/RIU. This high sensitivity of the H-shaped graphene structure to the dielectric substrate is of potential interest for plasmon sensors.

Moreover, we also investigate the PIT effect of the x axial symmetric H-shaped structure at different values of polarization angles θ, and the results are shown in Fig. 7. The schematic structure is shown in the inset of Fig. 7(a), where the left arm is shorter than the right arm and the central bar is located in the middle. The calculated transmission spectra are shown in Fig. 7(a) and the electric field distribution and surface current distribution at the resonant peak are shown in Figs. 7(b)–7(d), when $\theta = 90°$. From Fig. 7(a), it can be clearly found that a significant PIT effect can be achieved when the polarization angle θ approaches to 90°. With the increase of the θ, the high frequency transmission window gradually emerges. The electric field distribution and the sur-

face current distribution reveal the origin of the PIT effect. For the resonant frequency at 2.01 THz, only the long arm is excited strongly by the incident light, whereas the short arm is excited very weakly, as shown in Fig. 7(b). However, when the resonant frequency is 2.63 THz, only the short arm is excited strongly in Fig. 7(d). Both of the two arms are excited simultaneously on account of the resonance detuning at the resonant frequency 2.3 THz, as shown in Fig. 7(c). Moreover, due to the detuning of the resonance frequency, the strength of the induced electric field of the two arms at the transparency peak 2.3 THz is smaller than those of the two transmission dips at 2.01 THz and 2.63 THz. Comparing with the y axial symmetric H-shaped structure, we can find the difference between the two structures results in the PIT effect. For the former, toroidal currents induced by the incident field lead to two magnetic dipole moments giving rise a magnetic response in the system when $\theta = 0°$. For the latter, two arms coupled with the incident field results in two electric dipoles, but they are detuned with each other due to the opposite current oscillations of two arms when $\theta = 90°$.

Now we come to investigate the dependence of the absorption spectrum on Fermi energy for the x axial symmetric H-shaped structure. The contour of Fermi energy ranging from 0.5 eV to 0.8 eV versus frequency of the designed structure is plotted in Fig. 8 with $\theta = 90°$. It can be observed that the increase of Fermi energy induces the resonant peaks to be blue-shifted and the amplitudes of two dips to increase.

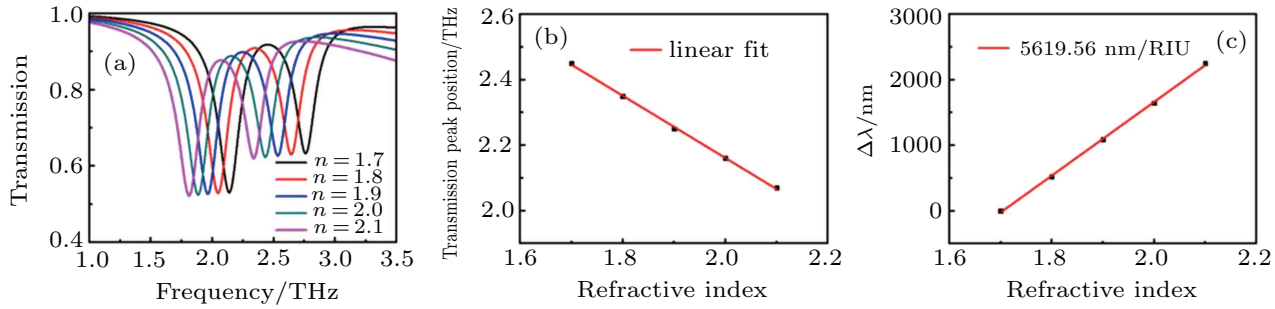


Fig. 6. (color online) (a) Transmission spectra of graphene-based PIT structure at different values of refractive index n, with $\theta = 0°$ and $E_F = 0.5$ eV, (b) relationship of the resonant PIT peak and refractive index n, and (c) relation between spectral shift $\Delta\lambda$ of the transparency peak and refractive index n of substrate.

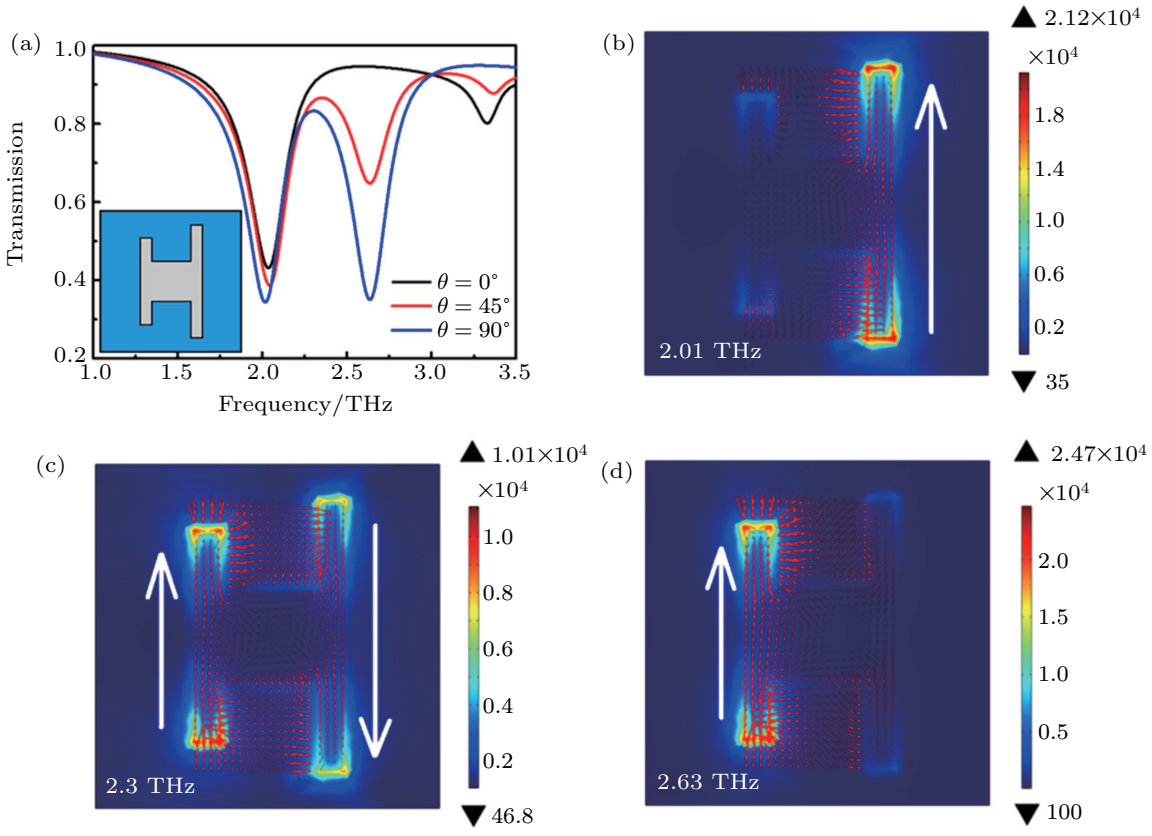


Fig. 7. (color online) (a) Transmission spectra of x-axial symmetric H-shaped structure at different values of polarization angle θ, and (b)–(d) electric field and surface current distribution at 2.01 THz, 2.3 THz, and 2.63 THz with $\theta = 90°$.

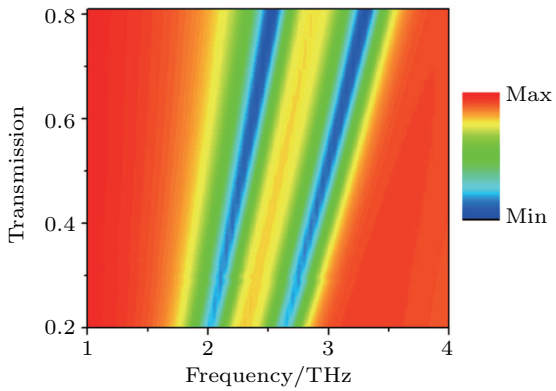


Fig. 8. (color online) Contour of Fermi energy versus frequency of *x*-axial symmetric H-shaped structure.

Graphene is an attractive 2D carbon material.[41] The carbon-to-carbon in-plane bond in graphene is very strong, which makes graphene sheets quite robust. However, carbon atom vacancies with respect to what would be a perfect armchair around the edge appears difficult to avoid.[42–44] We calculate the transmission spectrum and electric field distribution of the asymmetric H-shaped graphene structure with rough edges. The transmission spectrum of rough edge structure is simulated and compared with that of smooth edge structure in Fig. 9. The results illustrate that our structure with rough edges also achieves a typical PIT phenomenon. It is also found that the variation trends of the two curves are similar and the locations of the wave peaks vary slightly. The electric field and normalized surface current distributions at three different resonant positions are also presented. Figure 10(a) is the first resonant position at 1.96 THz. Figure 10(b) shows the second resonant position at 2.3 THz, and figure 10(c) displays the third resonant position at 2.53 THz. The results have similar distributions to those of the original structure in Fig. 3.

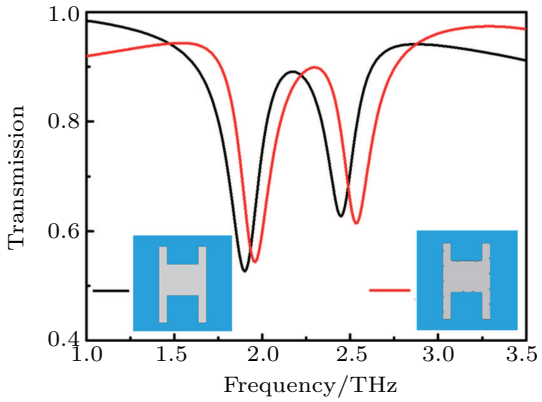


Fig. 9. (color online) Transmission spectra of smooth H-shaped asymmetric graphene structure (black line) and H structure with rough edges (red line) of the graphene-based structure at 0° polarization angle.

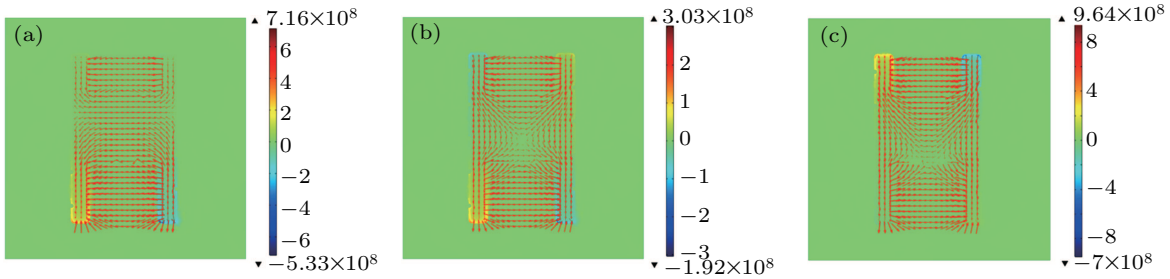


Fig. 10. (color online) The electric field and normalized surface current distributions of the rough asymmetric H shaped graphene structure at 0° polarization angle at three different resonant positions: (a) the first resonant position at 1.96 THz, (b) the second resonant position at 2.3 THz, and (c) the third resonant position at 2.53 THz.

4. Conclusions

In this work, we theoretically investigate the dynamically controllable PIT effect with two kinds of asymmetric H-shaped graphene resonators by varying polarization angles rather than changing the structure parameters. The transition from the switch-on state (PIT mode) to switch-off state (dipole mode) is theoretically demonstrated by simply adjusting the polarization angle. Importantly, the destructive interference between a dark mode and a bright mode is employed to analyze the transmission mechanism. The PIT resonance frequency can be dynamically tuned by adjusting the Fermi energy of the graphene, instead of re-fabricating the structures. The tunable PIT effect of the *x* axis symmetric H-shaped structure by the polarization angle is also investigated. The physical mechanism of the induced transparency is revealed from the electric dipole hybridization coupling. Moreover, our proposed asymmetric H-shaped graphene structures with rough edges can also embody the PIT effect. Based on the observed phenomenon, our designed H-shaped structures could offer new opportunities for applications in optical filter, optical sensors, and switches.

References

[1] Boller K J, Imamoglu A and Harris S E 1991 *Phys. Rev. Lett.* **66** 2593
[2] Harris S E 1997 *Phys. Today* **50** 36
[3] Fleischhauer M, Physik F, Kaiserslautern D, Imamoglu A and Marangos J P 2005 *Rev. Mod. Phys.* **77** 633
[4] Francesco M and Andrea A 2014 *Chin. Phys. B* **23** 047809
[5] Wang X X, Sun J X, Sun Y H, Li A J, Chen Y, Zhang X J, Kang Z H, Wang L, Wang H H and Gao J Y 2015 *Chin. Phys. B* **24** 074204
[6] Liu N, Langguth L, Weiss T, Kästel J, Fleischhauer M, Pfau T and Giessen H 2009 *Nat. Mater.* **8** 758
[7] Luk'yanchuk B, Zheludev N I, Maier S A, Halas N J, Nordlander P, Giessen H and Chong C T 2010 *Nat. Mater.* **9** 707
[8] Liu N, Weiss T, Mesch M, Langguth L, Eigenthaler U, Hirscher M, Sönnichsen C and Giessen H 2010 *Nano Lett.* **10** 1103

[9] Yu Z, Chen H, Liu J J, Jing X F, Li X J and Hong Z 2017 *Chin. Phys. B* **26** 077804

[10] Zhang Y D, Li J, Li H Y, Yao C B and Yuan P 2013 *Opt. Laser Technol.* **49** 202

[11] Novikova I, Walsworth R L and Xiao Y H 2012 *Laser Photon. Rev.* **6** 333

[12] He J N, Wang J Q, Ding P, Fan C Z, Arnaut L R and Liang E J 2015 *Plasmonics* **10** 1115

[13] Chen J X, Wang P, Chen C C, Lu Y H, Ming H and Zhan Q W 2011 *Opt. Express* **19** 5970

[14] Safavi-Naeini A H, Alegre T M, Chan J, Eichenfield M, Winger M, Lin Q, Hill J T, Chang D E and O 2011 *Nature* **472** 69

[15] Wang L, Cai W, Zhang X Z, Liu P H, Xiang Y X and Xu J J 2013 *Appl. Phys. Lett.* **103** 041604

[16] TianY C, Ding P and Fan C Z 2017 *Opt. Eng.* **56** 107106

[17] Li H J, Wang L L, . Liu J Q and Huang Z R 2013 *Appl. Phys. Lett.* **103** 211104

[18] Luo X, Qiu T, Lu W and Ni Z 2013 *Mater. Sci. Eng. R* **74** 351

[19] Zhang W X, Liu Y X, Tian H, Xu J W and Feng L 2015 *Chin. Phys. B* **24** 076104

[20] Vakil A and Engheta N 2011 *Science* **332** 1291

[21] Koppens F H, Chang D E, Thongrattanasiri S and Garcia F J G 2011 *Nano Lett.* **11** 3370

[22] Fu G L, Zhai X, Li H J, Xia S X and Wang L L 2017 *J. Opt.* **19** 015001

[23] Fu G L, Zhai X, Li H J, Xia S X and Wang L L 2016 *Plasmonics* **11** 1597

[24] Luo W W, Cai W, Xiang Y X, Wang L, Ren M X, Zhang X Z and Xu J J 2016 *Opt. Express* **24** 5784

[25] Niu Y Y, Wang J C, Hu Z D and Zhang F 2018 *Opt. Commu.* **416** 77

[26] Thongrattanasiri S, Koppens F H and Garcia F J 2012 *Phys. Rev. Lett.* **108** 047401

[27] Yao Y, Kats M A, Genevet P, Yu N F, Song Y, Kong J and Capasso F 2013 *Nano Lett.* **13** 1257

[28] Falkovsky L A and Pershoguba S S 2007 *Phys. Rev. B* **76** 153410

[29] Gusynin V P, Sharapov S G and Carbotte J P 2007 *J. Phys.: Condens. Matter* **19** 249

[30] Jablan M, Buljan H and Soljačić M 2009 *Phys. Rev. B* **80** 245435

[31] Hanson G W 2008 *J. Appl. Phys.* **103** 064302

[32] Novoselov K S, Geim A K, Morozov S V, Jiang D, Zhang Y, Dubonos S V, Grigorieva I V and Firsov A A 2004 *Science* **306** 666

[33] Liu C, Liu P, Yang C and Lian B 2017 *J. Opt.* **19** 115102

[34] Han M Y, Ozyilmaz B, Zhang Y and Kim P 2007 *Phys. Rev. Lett.* **98** 206805

[35] Wu Y Q, Ye P D, Capano M A, Xuan Y, Sui Y, Qi M, Cooper J A, Shen T, Pandey D, Prakash G and Reifenberger R 2008 *Appl. Phys. Lett.* **92** 092102

[36] Hu H, Zhai F, Hu D B, Li Z J, Bai B, Yang X X and Dai Q 2015 *Nanoscale* **7** 19493

[37] Fang Z Y, Thongrattanasiri S, Schlather A, Liu Z, Ma L L, Wang Y M, Ajayan P M, Nordlander P, Halas N J and Javier Garcia de Abajo F 2013 *ACS Nano* **7** 2388

[38] Yang R, Zhang L, Wang Y, Shi Z, Shi D, Gao H, Wang Y and Zhang G 2010 *Adv. Mater.* **22** 4014

[39] Liu N, Kaiser S and Giessen H 2008 *Adv. Mater.* **20** 4521

[40] Singh R, Plum E, Menzel C, Rockstuhl C, Azad A K, Cheville R A, Lederer F, Zhang W and Zheludev N I 2009 *Phys. Rev. B* **80** 153104

[41] Ju L, Geng B, Horng J, Girit C, Martin M, Hao Z, Bechtel H A, Liang X G, Zettl A, Shen Y R and Wang F 2011 *Nat. Nano* **6** 630

[42] Basu D, Gilbert M J, Register L F and Banerjee S K 2008 *Appl. Phys. Lett.* **92** 042114

[43] Banadaki Y M and Srivastava A 2016 *Electronics* **5** 11

[44] Wadhwa P, Kumar S, Kumar T J D, Shukla A and Kumar R 2018 *J. Appl. Phys.* **123** 161416